

3-D Drone-Base-Station Placement with In-Band Full-Duplex Communications

© 2018 IEEE. Personal use of this material is permitted. Permission from IEEE must be obtained for all other uses, in any current or future media, including reprinting/republishing this material for advertising or promotional purposes, creating new collective works, for resale or redistribution to servers or lists, or reuse of any copyrighted component of this work in other works.

This material is presented to ensure timely dissemination of scholarly and technical work. Copyright and all rights therein are retained by authors or by other copyright holders. All persons copying this information are expected to adhere to the terms and constraints invoked by each author's copyright. In most cases, these works may not be reposted without the explicit permission of the copyright holder.

Citation:

L. Zhang, Q. Fan and N. Ansari, "3-D Drone-Base-Station Placement with In-Band Full-Duplex Communications," in *IEEE Communications Letters*, to be published.
doi: 10.1109/LCOMM.2018.2851206

URL:

<https://ieeexplore.ieee.org/document/8399887/>

3-D Drone-Base-Station Placement with In-Band Full-Duplex Communications

Liang Zhang, Qiang Fan, and Nirwan Ansari

Abstract—Drone-base-stations (DBSs) can potentially provision low-cost and flexible networking with high mobility while in-band full-duplex (IBFD) can conceivably improve spectrum efficiency. It is therefore logical to employ DBSs with IBFD in a cellular network to improve the network throughput. We decompose this problem into the DBS placement problem and the joint bandwidth and power allocation problem, and propose two heuristic algorithms to solve the whole problem. Simulation results have demonstrated that the total throughput of the Dynamic Drone-base-Station Placement (Dynamic-DSP) algorithm achieves up to 45% improvement as compared to that of the strategy without DBSs.

Index Terms—Drone-base-station, wireless backhauling, full-duplex, self-interference, backhaul interference.

I. INTRODUCTION

DBSs can be deployed to provide wireless services with high mobility and low cost [1]. Drone cells are especially useful for provisioning communications for temporary or unexpected events in sports, traffic jams, and emergency communications [2], [3]. DBSs can be used to overcome terrestrial BS failures, offload traffic from a congested macro base station (MBS), provide service to remote areas [4], and improve Quality of Service (QoS) of user equipments (UEs) [5].

Fig. 1(a) shows a DBS assisted half-duplex (HD) cellular network, where separate frequency spectra are employed in the backhaul link (from the MBS to a DBS) and access link (from the DBS to the UE), but the spectrum efficiency of HD is low. In contrast, in-band full-duplex (IBFD) can potentially double the spectrum efficiency as compared to HD [6]. IBFD enables simultaneous communications in the backhaul link and access link in the same frequency band [7]. However, it is difficult to transmit and receive data on the same frequency owing to severe self-interference (SI). Recent advances in SI cancellation, which can reduce SI by up to 150 dB [8], have enabled IBFD [7].

Kalantari *et al.* [4] addressed the DBS placement problem by maximizing the number of UEs covered by the DBS, and Sun *et al.* [5] minimized the total average latency ratio incurred by BSs; Wang *et al.* [9] determined the optimal drone position that minimizes the transmission power in provisioning a set of UEs; Goyal *et al.* [6] maximized the total average data rate of either downlink or uplink for FD enabled small base stations (SBSs); Siddique *et al.* [7] maximized the overall achievable rates of SBSs via access/backhaul spectrum allocation while considering both IBFD and out-of-band FD backhauling. Since

IBFD can significantly improve the throughput of the DBS assisted cellular network, we formulate the Drone-base-Station Placement with In-Band Full-Duplex communication (DSP-IBFD) problem, which includes the DBS placement problem, and the bandwidth and power allocation (in the access link and the backhaul link) problem. We propose two heuristic algorithms based on different DBS placement strategies to solve the DSP-IBFD problem. One is the fixed DBS placement (benchmark), and the other is the dynamic DBS placement, which aims to achieve better performance. Meanwhile, the bandwidth and power allocation are optimized based on the DBS placement results.

II. SYSTEM MODEL

We consider a heterogeneous network (HetNet) consisting of a MBS (HD-enabled) and a few DBSs (IBFD-enabled) deployed as small cells. Fig. 1(b) shows the backhaul link and access link of a DBS sharing the same frequency. Meanwhile, different DBSs use different frequency spectra, thus not incurring BS-BS interference between each other. A UE associated with a DBS receives the interference from the backhaul link from the MBS to their DBS, which is different from Fig. 1(a).

Denote $\mathcal{B} = \{1, 2, \dots, k\}$ as the BS set, where $\mathcal{B}' = \{j \in \mathcal{B}, j \neq 1\}$ is the DBS set, and $j = 1$ refers to the MBS. $\mathcal{U} = \{u_1, u_2, \dots, u_n\}$ is the UE set. We consider a MBS of coverage radius C_m overlapped with multiple DBSs. At the beginning, DBSs are located at the MBS, and then move to the target area, hovering there to provide services to UEs. We consider low-mobility DBSs (DBSs are hovering most of the time); both the MBS and DBSs dynamically allocate power and bandwidth to UEs. In this letter, we only focus on downlink communications from the MBS to UEs via a DBS or from the MBS to UEs.

A. Path Loss Model

When DBSs communicate with UEs on the ground, two types of path loss are considered, i.e., line-of-sight (LoS) and non-line-of-sight (NLoS) [4], [10].

Probabilities of a LoS (Ψ_L) and NLoS (Ψ_N) transmission between a transmitter and a receiver are expressed in Eq. (1). Here, a and b are constants, which are determined by the environment (rural, urban, etc.), $\theta = \arctan(\frac{h}{r})$ is the elevation angle, h is the altitude of a DBS, and r is the horizontal distance, respectively [4], [11].

$$\begin{cases} \Psi_L = [1 + a * \exp(-b(\frac{180\theta}{\pi} - a))]^{-1} \\ \Psi_N = 1 - \Psi_L \end{cases} \quad (1)$$

Since it is difficult to determine the exact LoS or NLoS of a connection between a user and a DBS, we use the mean path

Liang Zhang, Qiang Fan and Nirwan Ansari are with the Advanced Networking Lab. Dept. Elec. & Comp. Engrg., New Jersey Institute of Technology, Newark, NJ, 07102, USA. Email: {lz284, qf4, nirwan.ansari}@njit.edu

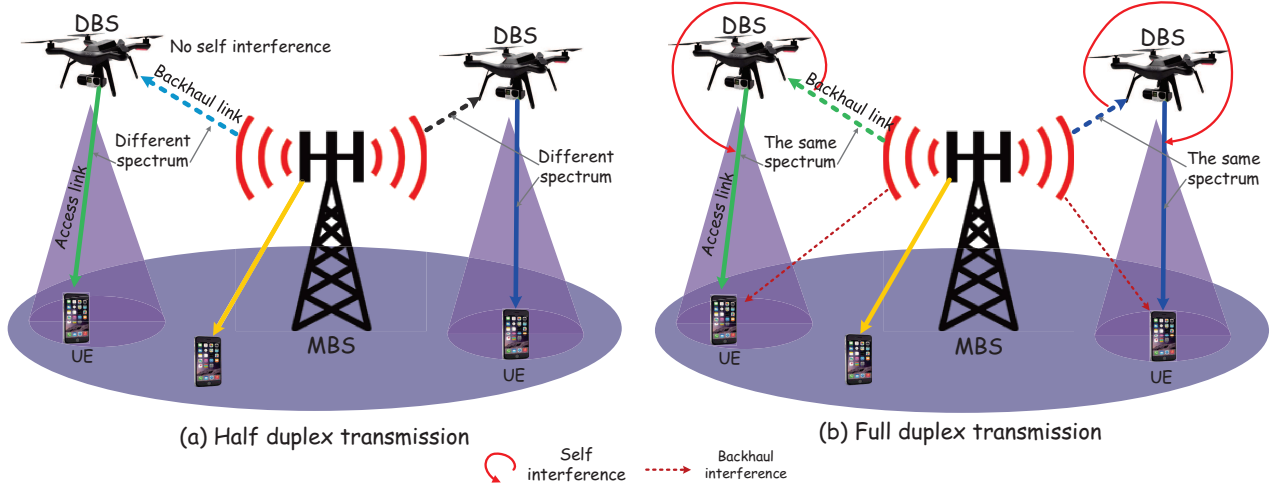


Fig. 1. Half duplex and full duplex communications with DBSs.

loss Γ instead of the exact path loss of the LoS or NLoS, as detailed in Eq. (2). Here, η_L and η_N are the additional mean losses of LoS and NLoS links, f_c is the carrier frequency, c is the speed of light, and $d = \sqrt{(h^2 + r^2)}$ is the distance between a DBS and a UE [4].

$$\Gamma = \eta_L \Psi_L + \eta_N \Psi_N + 20 \log(4\pi f_c d / c) \quad (2)$$

After substituting Ψ_L and Ψ_N into Eq. (2), we can transform Eq. (2) into Eq. (3). As a result, Γ is a function of h and r , implying that the path loss is a function of the altitude and coverage of the DBS. For a given Γ , the coverage radius r of a DBS is a function of its altitude h . Note that $20 \log(4\pi f_c d / c) = 20 \log(4\pi f_c / c) + 20 \log(r / \cos \theta)$.

$$\Gamma = \frac{\eta_L - \eta_N}{1 + a * \exp(-b(\frac{180 * \theta}{\pi} - a))} + 20 \log(\frac{4\pi f_c d}{c}) + \eta_N \quad (3)$$

B. Communications Model

We assume the transmit power-spectral density of each BS is constant [12]. Let $p_{i,j}$ and $b_{i,j}$ be the allocated power and frequency bandwidth for the i th UE of the j th BS (note that each UE is associated with only one BS); denote $s_{i,j}$ as the signal to interference plus noise ratio (SINR) of the i th UE towards the j th BS, as detailed in Eq. (4).

$$s_{i,j} = \begin{cases} \frac{p_{i,j} |h_{i,j}|^2}{\sigma^2}, & j = 1 \\ \frac{p_{i,j} \Gamma_{i,j}}{p_{i,j'} |h_{i,j'}|^2 + \sigma^2}, & j \in \mathcal{B}', j' = 1 \end{cases} \quad (4)$$

Here, $h_{i,j}$ is the channel gain between the k th BS and the i th UE; $\Gamma_{i,j}$ is the path loss of the i th UE when it is associated with the j th ($j > 1$) DBS; $\sigma^2 = b_{i,j} * N_0$ is the thermal noise power, and N_0 is the thermal noise power spectral density.

Let $\phi_{i,j}$ be the data rate of the i th UE from the j th BS. Then, a UE's data rate is determined by $s_{i,j}$ and $b_{i,j}$ according to the Shannon Hartley theorem [13], as shown in Eq. (5). To reduce the problem complexity, we assume $p_{i,j} = b_{i,j} * \zeta_j$, where ζ_j is the power-spectral density [14]. Then, we only need to allocate the bandwidth for each UE.

$$\phi_{i,j} = b_{i,j} \log_2(1 + s_{i,j}) \quad (5)$$

There are two types of interferences in our network: SI at the DBS, and backhaul interference [6], [7]; DBSs will experience

SI, and a UE associated with a DBS will be affected by the transmission power of the backhaul from the MBS to this DBS. Then, the data rate of the backhaul f_j is formulated as Eq. (6).

$$f_j = \beta_B \log_2(1 + \frac{P_{1,j} \Gamma_{1,j}}{I_{SI} + \sigma_j^2}), \quad j \in \mathcal{B}' \quad (6)$$

Here, $P_{1,j}$ is the transmission power from the MBS to the j th DBS; $\Gamma_{1,j}$ is the path loss from the MBS to the j th DBS (by Eq. (2)); β_B is the total backhaul bandwidth for a DBS, which is reused by both the DBS's backhaul link and its access links towards UEs (β_B is set to 3.3 MHz in the simulation); $\sigma_j^2 = \beta_B * N_0$ is the thermal noise power; N_0 is the thermal noise power spectral density; $I_{SI} = \sum_i p_{i,j} / C_{SI}$ is the residual SI experienced at the DBS, and $1/C_{SI}$ is the residual self-interference power [7].

III. PROBLEM FORMULATION

After the locations of all DBSs are determined, each UE is associated with the BS that has the highest SINR.

Notations (given):

N : the number of DBS, $N = |\mathcal{B}'|$.

x_i^{ue}, y_i^{ue} : the location of the i th UE.

P_M : the maximum transmission power of a MBS.

P_D : the maximum transmission power of a DBS.

d_{min} : the minimum data rate for each UE.

ζ_j : the power-spectral density of the j th BS.

$P_{j',j} (j' = 1)$: the transmission power of the MBS towards the j th DBS for the backhaul link.

Variables:

$\omega_{i,j}$: binary variable: 1 if the i th UE is associated with the j th BS; 0, otherwise.

$b_{i,j}$: the bandwidth of the j th BS allocated to the i th UE.

$p_{i,j}$: the transmission power of the j th BS allocated to the i th UE.

$\{x_j, y_j, h_j\}$: 3-D co-ordinates of the j th DBS; h_j is the altitude.

P_j : the total transmission power of the j th DBS towards its associated UEs, where $P_j = \sum_i b_{i,j} * \zeta_j * \omega_{i,j}$.

Φ_j : the total throughput of the j th BS, $\Phi_j = \sum_i \phi_{i,j}$.

The objective of the DSP-IBFD problem is to maximize the throughput of the whole network as expressed in Eq. (7).

$$\max_{x_j, y_j, h_j, \omega_{i,j}, b_{i,j}} \sum_j \Phi_j \quad (7)$$

s.t. :

$$\sum_j \omega_{i,j} = 1, \quad \forall i \in \mathcal{U} \quad (8)$$

$$\omega_{i,j^*} = 1, j^* = \arg_j(\max s_{i,j}), \quad \forall i \in \mathcal{U} \quad (9)$$

$$\sum_i \phi_{i,j} \leq f_j, \quad \forall j \in \mathcal{B}' \quad (10)$$

$$P_j \leq P_D, \quad \forall j \in \mathcal{B}' \quad (11)$$

$$\sum_i b_{i,j'} * \zeta_{j'} + \sum_{j,j' \neq j} P_{j',j} \leq P_M, \quad \forall j, j' = 1 \quad (12)$$

$$\phi_{i,j} \geq \omega_{i,j} * d_{min}, \quad \forall i \in \mathcal{U}, j \in \mathcal{B} \quad (13)$$

$$h_{min} \leq h_j \leq h_{max}, \quad \forall j \in \mathcal{B}' \quad (14)$$

Eq. (8) imposes each UE to be associated with only one BS, and Eq. (9) ensures that each UE is associated with the BS with the best SINR. Eq. (10) is the backhaul data rate capacity constraint, and it ensures that the total data rate of a DBS cannot exceed its backhaul capacity. Eq. (11) is the power constraint of each DBS, and it ensures that the total transmission power of a DBS towards its associated UEs should not exceed the maximum available power. Eq. (12) is the power constraint of the MBS, and it ensures that the aggregated transmission power of the MBS towards its associated UEs and all DBSs should not exceed the maximum available power. Eq. (13) is the minimum data rate constraint, and it ensures that each UE's data rate should exceed the minimum threshold when it is associated with a BS. Eq. (14) is the altitude constraint for a DBS, and it provides the lower bound and upper bound altitudes for placing the DBS, respectively.

IV. HEURISTIC ALGORITHM

The DSP-IBFD problem is a non-linear non-convex combinatorial optimization problem, which can be decomposed into the DBS placement problem and the resource allocation problem. The DBS placement problem is a set cover problem, which is NP-hard, and hence it is hard to find the optimal solution [6]. Hence, we propose two heuristic algorithms to solve this problem, namely, the Dynamic-DSP and Fixed-DSP algorithm.

The Dynamic-DSP algorithm is summarized in *Algorithm 1*. Here, Eq. (15) defines the weight of the i th UE for the DBS placement; we assume the coverage of the DBS is C_j , which is only used for the DBS placement; the maximum loop number L_{max} is used to iteratively find the resource allocation of the DBS, which best matches the backhaul capacity and the data rate of UEs' access links; ε is a given small deviation value. Each BS provides the minimum data rate (500 kbps) to all associated UEs first, and the remaining power and bandwidth are then assigned to the UE which has the highest SINR to achieve the highest throughput. We first find the locations to place all DBSs (*Lines 1-5*), and then get the UE association and allocate bandwidth and power to UEs associated with the MBS (*Lines 6-8*). Afterwards, power and

Algorithm 1: Dynamic-DSP Algorithm

Input : (x_i^{ue}, y_i^{ue}) and other parameters in Table I;
Output: $\{x_j, y_j, h_j\}, \omega_{i,j}, b_{i,j}$;

- 1 **for** $j \in \mathcal{B}'$ **do**
- 2 calculate the weight of UEs in C_j by Eq. (15);
- 3 get x_j and y_j with the highest weight;
- 4 remove UEs in the coverage of the j th DBS;
- 5 calculate SINR of all UEs and all BSs;
- 6 get h_j with the best average SINR of all UEs;
- 7 calculate the UE association based on the best SINR;
- 8 allocate the bandwidth and power to UEs in MBS according to Eq. (13);
- 9 assign the redundant bandwidth and power to the UE which has the best SINR in MBS;
- 10 $L = 0, D = 1, D_j = 1, P_j^L = P_D/2^{L+1}, \forall j$;
- 11 **while** $D > 0$ & $L < L_{max}$ **do**
- 12 set maximum available power $P_j^{max} = \sum P_j^L, \forall j$;
- 13 **for** $j \in \mathcal{B}'$ **do**
- 14 allocate the bandwidth and power to UEs by Eq. (13);
- 15 assign the remaining bandwidth and power to the UE which has the best SINR;
- 16 **if** $|\sum_i \phi_{i,j} - f_j|/f_j < \varepsilon$ **then**
- 17 $D_j = 0$, and $D = \sum_j D_j$;
- 18 **continue**;
- 19 **if** $\sum_i \phi_{i,j} \geq f_j$ **then**
- 20 set $P_j^{L+1} = P_D/2^{(L+1)+1}$;
- 21 **else**
- 22 set $P_j^{L+1} = -P_D/2^{(L+1)+1}$;
- 23 $L = L + 1$, and $D = \sum_j D_j$;
- 24 update $b_{i,j} = p_{i,j}/\zeta_j, \omega_{i,j}$, and P_j ;

bandwidth of each DBS are allocated to its associated UEs such that the aggregated data rate of these UEs is close to the DBS's backhaul capacity (*Lines 9-22*). The complexity of Steps 1-4 is $O(C_m/C_j|U||B|)$; that of Steps 5-6 is $O((h_{max} - h_{min})/\Delta h|B|)$, where Δh is the increment of the altitude used in the iteration; that of Step 7 is $O(|U|^{|B|})$; that of Steps 12-23 is $O(|B|(|U| + \log(|U|)))$, and they can repeat for at most L_{max} times in the worst case. Thus, the complexity of Steps 11-23 can reach $O(L_{max}|B|(|U| + \log(|U|)))$. Therefore, the complexity of the Dynamic-DSP algorithm is $O(C_m/C_j|U||B| + (h_{max} - h_{min})/\Delta h|B| + |U|^{|B|} + L_{max}|B|(|U| + \log(|U|)))$.

$$\xi_i = 1 + ((x_i^{ue} - x_j)^2 + (y_i^{ue} - y_j)^2)^{-1} \quad (15)$$

For the Fixed-DSP algorithm, we place all DBS in fixed locations, and then execute *Lines 6 – 22* in *Algorithm 1*.

V. PERFORMANCE EVALUATION

In this paper, we consider three DBSs and one MBS ($|\mathcal{B}'| = 3$) in an urban area (i.e., the coverage area of the MBS is $500 * 500 m^2$). The frequency spectra of all BSs are around $f = 2$ GHz. We set the maximum transmission power of a DBS as $P_D = 1$ W, and that of the MBS as $P_M = 4$ W. The remaining parameters, such as a, b, η_L , and η_N , are listed in Table I [4].

Fig. 2 shows the network throughput achieved by the Dynamic-DSP and the Fixed-DSP algorithms for different altitudes where the total number of UEs in the network is

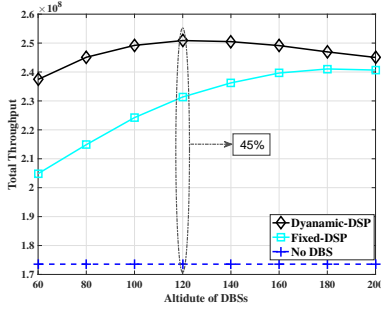


Fig. 2. Performance with 100 UEs.

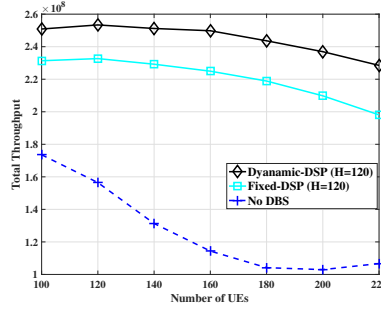


Fig. 3. Performance with fixed altitude.

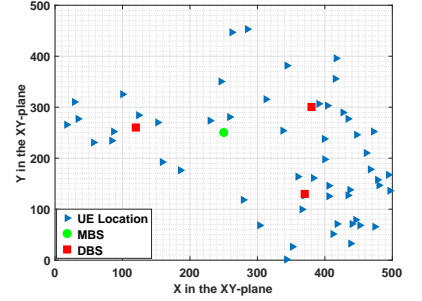


Fig. 4. DBS placement by Dynamic-DSP.

TABLE I
SIMULATION PARAMETERS

a , environment constant	9.61
b , environment constant	0.16
η_L , additional mean loss of LoS	1 dB
η_N , additional mean loss of NLoS	20 dB
C_m , MBS cell coverage	$500 * 500 m^2$
C_j , coverage of a DBS (used for DBS placement)	$70 * 70 m^2$
h_{min} , the minimum altitude of a DBS	60 m
h_{max} , the maximum altitude of a DBS	200 m
path loss of MBS-UE	$34.5 + 35 * \log_{10}(d[m])$ [12]
Shadow fading of MBS-UE	$N(0, 8^2)$ dB
N_0 , thermal noise power spectral density	-174 dBm/Hz
C_{SI} , SI cancellation value	130 dB [8]
β_M , the total bandwidth capacity of the MBS	20 MHz
β_B , the total backhaul bandwidth of a DBS	3.3 MHz
P_M , the maximum transmission power of a MBS	4 W
P_D , the maximum transmission power of a DBS	1 W
$ U $, the number of UEs	{100, 120, ..., 220}
The minimal data rate	500 kbps
L_{max} , the maximum loop number	60
ϵ , deviation of throughput and backhaul data rate	0.0002

100. The throughput achieved by the Dynamic-DSP strategy has been increased by 45% and 8% as compared to the strategy without DBS and the Fixed-DSP strategy, respectively. The throughput increases as the altitude increases. The NLoS path loss between a DBS and its associated UEs degrades with the increasing altitude of the DBS. Then, the network throughput decreases when the altitude is more than 120m because when the altitudes of DBSs are very high, the distances between UEs and DBSs become the dominant factor for the path loss, thus degrading the throughput of the network.

Fig. 3 shows the network throughput when DBSs hover at the altitude of 120m as the number of UEs varies; both of the proposed strategies can provide a higher throughput as compared to the one without DBSs because the two proposed strategies can place DBSs close to UEs to improve the SINR of UEs. The throughput without DBSs decreases as the number of UEs increases because the MBS needs to allocate most bandwidth to UEs with bad channel conditions to maintain their minimum data rates, and thus the bandwidth allocated to UEs with high SINR is reduced. Fig. 4 shows how DBSs are placed by Dynamic-DSP; note that DBSs hover close to regions with higher UE densities but not far away from the MBS.

VI. CONCLUSION

We have investigated the drone-base-station placement with IBFD communications (DSP-IBFD) problem, which is a non-

linear non-convex combinatorial optimization problem, and can be decomposed into the DBS placement problem and the joint bandwidth and power allocation problem. We have proposed two heuristic algorithms based on different DBS placement strategies to solve the DSP-IBFD problem. Simulation results have demonstrated that the network throughput achieved by Dynamic-DSP is 45% and 8% more than that of without DBSs and that by the Fixed-DSP strategy, respectively.

REFERENCES

- [1] Y. Zeng, R. Zhang, and T. J. Lim, "Wireless communications with unmanned aerial vehicles: opportunities and challenges," *IEEE Communications Magazine*, vol. 54, no. 5, pp. 36–42, May 2016.
- [2] I. Bor-Yaliniz and H. Yanikomeroglu, "The new frontier in RAN heterogeneity: Multi-tier drone-cells," *IEEE Communications Magazine*, vol. 54, no. 11, pp. 48–55, Nov. 2016.
- [3] Z. Kaleem and M. H. Rehmani, "Amateur drone monitoring: State-of-the-art architectures, key enabling technologies, and future research directions," *IEEE Wireless Communications*, vol. 25, no. 2, pp. 150–159, Apr. 2018.
- [4] E. Kalantari, M. Z. Shakir, H. Yanikomeroglu, and A. Yongacoglu, "Backhaul-aware robust 3D drone placement in 5G+ wireless networks," in *Proc. ICC Workshops*, pp. 1–6, May 2017.
- [5] X. Sun and N. Ansari, "Latency aware drone base station placement in heterogeneous networks," in *Proc. IEEE GLOBECOM*, pp. 1–6, Dec. 2016.
- [6] S. Goyal, P. Liu, and S. S. Panwar, "User selection and power allocation in full-duplex multicell networks," *IEEE Transactions on Vehicular Technology*, vol. 66, no. 3, pp. 2408–2422, Mar. 2017.
- [7] U. Siddique, H. Tabassum, and E. Hossain, "Downlink spectrum allocation for in-band and out-band wireless backhauling of full-duplex small cells," *IEEE Transactions on Communications*, vol. 65, no. 8, pp. 3538–3554, Aug. 2017.
- [8] Y. S. Choi and H. Shirani-Mehr, "Simultaneous transmission and reception: Algorithm, design and system level performance," *IEEE Transactions on Wireless Communications*, vol. 12, no. 12, pp. 5992–6010, Dec. 2013.
- [9] L. Wang, B. Hu, and S. Chen, "Energy efficient placement of a drone base station for minimum required transmit power," *IEEE Wireless Communications Letters*, pp. 1–1, Feb. 2018.
- [10] A. Al-Hourani, S. Kandeepan, and A. Jamalipour, "Modeling air-to-ground path loss for low altitude platforms in urban environments," in *IEEE GLOBECOM*, pp. 2898–2904, Dec. 2014.
- [11] A. Al-Hourani, S. Kandeepan, and S. Lardner, "Optimal lap altitude for maximum coverage," *IEEE Wireless Communications Letters*, vol. 3, no. 6, pp. 569–572, Dec. 2014.
- [12] Q. Fan and N. Ansari, "Green energy aware user association in heterogeneous networks," in *IEEE Wireless Communications and Networking Conference*, pp. 1–6, Apr. 2016.
- [13] X. Huang, T. Han, and N. Ansari, "Smart grid enabled mobile networks: Jointly optimizing BS operation and power distribution," *IEEE/ACM Transactions on Networking*, vol. 25, no. 3, pp. 1832–1845, Jun. 2017.
- [14] T. Han and N. Ansari, "Enabling mobile traffic offloading via energy spectrum trading," *IEEE Transactions on Wireless Communications*, vol. 13, no. 6, pp. 3317–3328, Jun. 2014.